JOC Article

Nonmevalonate Terpene Biosynthesis Enzymes as Antiinfective Drug Targets: Substrate Synthesis and High-Throughput Screening Methods

Victoria Illarionova,† Johannes Kaiser,* Elena Ostrozhenkova, Adelbert Bacher, Markus Fischer, Wolfgang Eisenreich,* and Felix Rohdich*

Lehrstuhl für Organische Chemie und Biochemie, Department Chemie, Technische Universität München, Lichtenbergstrasse 4, D-85747 Garching, the Institut für Biochemie und Lebensmittelchemie, Abteilung Lebensmittelchemie, Universität Hamburg, Grindelallee 117, 20146 Hamburg, Germany, and the Ikosatec GmbH, Königsberger Strasse 74, D-85748 Garching, Germany

felix.rohdich@ch.tum.de

Received July 14, 2006

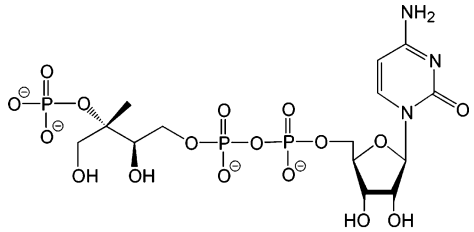

4-Diphosphocytidyl-2*C*-methyl-D-erythritol 2-phosphate

The nonmevalonate isoprenoid pathway is an established target for antiinfective drug development. This paper describes high-throughput methods for the screening of 2*C*-methyl-D-erythritol synthase (IspC protein), 4-diphosphocytidyl-2*C*-methyl-D-erythritol synthase (IspD protein), 4-diphosphocytidyl-2*C*-methyl-D-erythritol kinase (IspE protein), and 2*C*-methyl-D-erythritol 2,4-cyclodiphosphate synthase (IspF protein) against large compound libraries. The assays use up to three auxiliary enzymes. They are all monitored photometrically at 340 nm and are robust as documented by *Z*-factors of ≥ 0.86. ^{13}C NMR assays designed for hit verification via direct detection of the primary reaction product are also described. Enzyme-assisted methods for the preparation, on a multigram scale, of isoprenoid biosynthesis intermediates required as substrates for these assays are reported. Notably, these methods enable the introduction of single or multiple ^{13}C labels as required for NMR-monitored assays. The preparation of 4-diphosphosphocytidyl-2*C*-methyl-D-erythritol 2-phosphate in multigram quantities is described for the first time.

Introduction

The tremendous success of antibiotic and antiparasitic agents developed in the wake of World War II has played an important role in the dramatic reduction of morbidity and mortality caused by infectious agents that we have witnessed in industrialized countries.[1] On the other hand, protozoan, bacterial, and viral infections continue to be the dominant factor of mortality on a worldwide basis.[2] Specifically, malaria is assumed to cause about 300 to 450 million infections per year with a death toll of several million, predominantly in the age group of children.[3] Moreover, one-third of the human population is reported to be infected with *Mycobacterium tuberculosis*, and tuberculosis causes at least one million deaths per year.[4]

Historically, the medical impact of antibiotics caused a state of complacency where morbidity and mortality due to infectious disease was played down.[5] This attitude has now been replaced by the awareness that every medically used antiinfective agent is subject to attrition by resistance development which typically begins within months or years after deployment.[6] One of the

* To whom correspondence should be addressed. Phone: +49-89-289-13364; +49-89-289-13336 (F.R.). Fax: +49-89-289-13363 (F.R.).
† On leave of absence from the Institute of Biophysics, Krasnoyarsk, Russia.

(1) Cohen, M. L. *Nature* **2000**, *406*, 762−767.
(2) Morens, D. M.; Folkers, G. K.; Fauci, A. S. *Nature* **2004**, *430*, 242−249.
(3) Hoffman, S. L.; Subramanian, G. M.; Collins, F. H.; Venter, J. C. *Nature* **2002**, *415*, 702−709.
(4) Wade, M. M.; Zhang, Y. *Front. Biosci.* **2004**, *9*, 975−994.
(5) Wenzel, R. P. *N. Engl. J. Med.* **2004**, *351*, 523−526.
(6) Service, R. F. *Science* **2004**, *303*, 1798.

10.1021/jo061466o CCC: $33.50 © 2006 American Chemical Society
Published on Web 10/18/2006

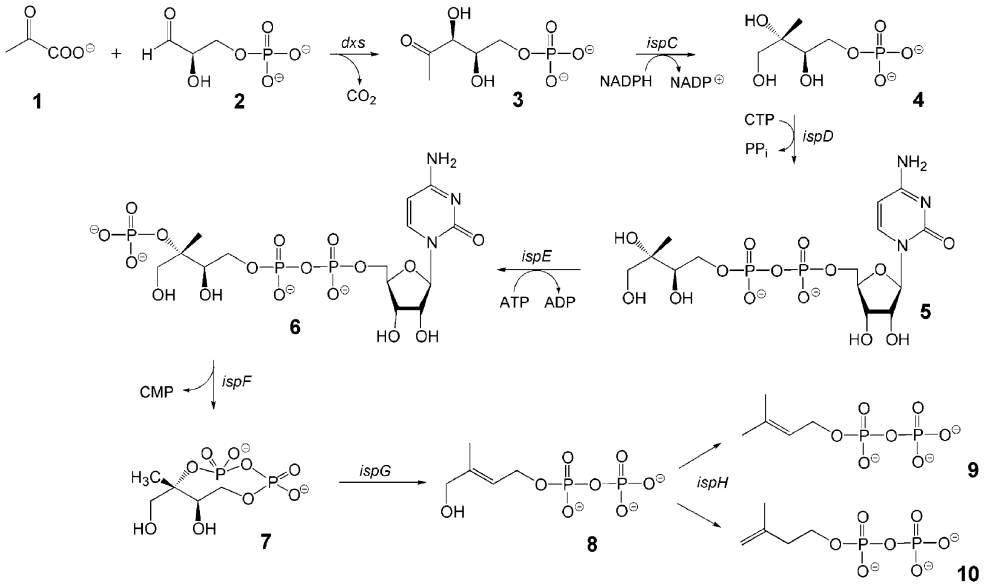

FIGURE 1. Nonmevalonate isoprenoid pathway.

most threatening aspects of this development is the emergence of multiresistant strains, for example of *M. tuberculosis*, *Staphylococcus aureus*, and *Plasmodium* spp.[4,7−9] Concern is also raised by the observation that phasing out of a specific antibiotic does not necessarily result in rapid decline of resistance in the bacterial population.[10−12] This came as a surprise since resistance mutations should be expected to cause at least some reduction in fitness that should favor the disappearance of the respective strain if the selective pressure is removed.[13] However, it is now clear that the loss of fitness due to resistance mutations can be compensated by secondary mutations at other sites.[14]

One would expect this state of matters to be conducive to a massive research effort directed at the development of novel antiinfective agents by the pharmaceutical industry. Contrary to that expectation, numerous pharmaceutical companies have outsourced or closed their antiinfective drug development departments.[15] Despite the apparent paradox, these developments reflect sound economic reasoning. Most antiinfective drugs are used for short periods only and are therefore at an economic disadvantage as compared to drugs directed at chronic conditions including cancer, cardiovascular, and neuropsychiatric disease. Moreover, a newly deployed antibiotic has to compete on the market against established compounds and is at the same time subject to attrition by resistance development. Last but not least, the medical community should try to restrict the use of any new drugs to patients suffering from infections by multiresistant pathogens in order to delay resistance development, but that would negatively influence the marketing success of the commercial product.[16]

Presently used antibiotics address only a relatively small number of molecular targets in the range of about 50.[17,18] Given the size of the genomes of parasitic bacteria and protozoa in the range of thousands of genes, one might optimistically assume that the number of targets available for future antiinfective research remains large. However, at this time, it is not possible to come up with a scientifically based estimate on the number of "druggable" antimicrobial targets. In any case, the target euphoria that characterized the period following the publication of the first bacterial genomes has been replaced by a less optimistic attitude.

The recently discovered nonmevalonate pathway of isoprenoid biosynthesis (Figure 1; for review, see refs 19−21) is a potential target for antiinfective drug development.[22] On the basis of the more than 600 completely sequenced genomes in public databases, it is now clear that the vast majority of pathogenic bacteria (with the exception of Gram-positive cocci including *Staphylococcus*, *Enterococcus*, and *Streptococcus* spp.) use this pathway for the biosynthesis of essential metabolic products including quinone cofactors required for respiration (for review, see refs 23 and 24). Moreover, the pathway is the unique source for isoprenoids in *Plasmodium* spp. causing

(7) Morlais, I.; Mori, A.; Schneider, J. R.; Severson, D. W. *Mol. Genet. Genomics* **2003**, *269*, 753−764.
(8) Alou, L.; Cafini, F.; Sevillano, D.; Unzueta, I.; Prieto, J. *Int. J. Antimicrob. Agents* **2004**, *23*, 513−516.
(9) Weigel, L. M.; Clewell, D. B.; Gill, S. R.; Clark, N. C.; McDougal, L. K.; Flannagan, S. E.; Kolonay, J. F.; Shetty, J.; Killgore, G. E.; Tenover, F. C. *Science* **2003**, *302*, 1569−1571.
(10) Bean, D. C.; Livermore, D. M.; Papa, I.; Hall, L. M. *J. Antimicrob. Chemother.* **2005**, *56*, 962−964.
(11) Bywater, R.; McConville, M.; Phillips, I.; Shryock, T. *J. Antimicrob. Chemother.* **2005**, *56*, 538−543.
(12) Grape, M.; Farra, A.; Kronvall, G.; Sundstrom, L. *Clin. Microbiol. Infect.* **2005**, *11*, 185−192.
(13) Cohen, T.; Becerra, M. C.; Murray, M. B. *Microb. Drug Resist.* **2004**, *10*, 280−285.
(14) Bjorkman, J.; Nagaev, I.; Berg, O. G.; Hughes, D.; Andersson, D. I. *Science* **2000**, *287*, 1479−1482.
(15) Service, R. F. *Science* **2004**, *303*, 1796−1799.
(16) Alekshun, M. N. *Expert. Opin. Invest. Drugs* **2005**, *14*, 117−134.
(17) Schmidt, F. R. *Appl. Microbiol. Biotechnol.* **2004**, *63*, 335−343.
(18) Gräfe, U. *Biochemie der Antibiotika: Struktur-Biosynthese-Wirkmechanismus*; Spektrum Akademischer Verlag: Heidelberg, Berlin, New York, 1992.
(19) Eisenreich, W.; Bacher, A.; Arigoni, D.; Rohdich, F. *Cell. Mol. Life Sci.* **2004**, *61*, 1401−1426.
(20) Rohmer, M.; Grosdemange-Billiard, C.; Seemann, M.; Tritsch, D. *Curr. Opin. Invest. Drugs* **2004**, *5*, 154−162.
(21) Rodríguez-Concepción, M. *Curr. Pharm. Des.* **2004**, *10*, 2391−2400.
(22) Bacher, A.; Eisenreich, W.; Fellermeier, M.; Fischer, M.; Hecht, S.; Herz, S.; Kis, K.; Lüttgen, H.; Rohdich, F.; Sagner, S.; Schuhr, C. A.; Wungsintaweekul, J.; Zenk, M. H. *Isoprenoid Biosynthesis*; International Patent Application No. WO2000EP, 07548, 2001.
(23) Rohdich, F.; Bacher, A.; Eisenreich, W. *Bioorg. Chem.* **2004**, *32*, 292−308.
(24) Rohdich, F.; Bacher, A.; Eisenreich, W. *Biochem. Soc. Trans.* **2005**, *33*, 785−791.

malaria.[25−27] The antibiotic fosmidomycin, which inhibits the first committed enzyme of the pathway,[28] has been reported to cure malaria in a clinical study.[27]

Optically monitored assays that are suitable, in principle, for high-throughput screening have been reported for IspC, IspD, and IspE protein.[29−31] This paper describes a platform with documented robustness for high-throughout screening of large compound libraries against IspCDEF proteins using a uniform concept with optical readout via the consumption of reduced pyrimidine nucleotides. We also describe assays designed to monitor the formation of target enzyme product directly by ^{13}C NMR spectroscopy which were specifically designed for hit verification. Enzyme-assisted methods for the preparation of the required substrates in multigram amounts, with or without ^{13}C labels in various positions that enable monitoring of enzyme reaction by ^{13}C NMR, are also reported.

Results

Enzyme-Assisted Preparation of Substrates. Chemical and/or enzyme-assisted procedures have been reported for the preparation, in millimole amounts, of the intermediates of the nonmevalonate isoprenoid pathway with the exception of 4-diphosphocytidyl-2*C*-methyl-D-erythritol 2-phosphate (**6**)[32−49] (for review, see also ref 19 (Figure 1)). Some of these procedures can be adapted to include labeling with stable or radioactive isotopes.

On the other hand, our initial attempts to prepare **6** by enzyme-assisted synthesis (Figure 2), in analogy to other intermediates of the pathway, met with limited success with regard to yield and purity. These difficulties prompted an investigation of the equilibrium constants of the reactions catalyzed by IspD and IspE protein. For this purpose, reaction mixtures containing relatively large amounts of IspD or IspE protein, to guarantee the rapid establishment of equilibrium, were monitored by ^{31}P NMR. It was favorable for that approach that **4**, **5**, ATP, ADP, CTP, and pyrophosphate afford characteristic ^{31}P NMR signals (Table 1); notably, the signals of **5**, ATP, ADP, CTP, and CDP show splitting by ^{31}P^{31}P coupling, and the characteristic coupling constants facilitate their unequivocal assignment. Moreover, some of the signals in ^{13}C-labeled **4** and **5** display ^{31}P^{13}C coupling that can be observed using appropriately ^{13}C-labeled samples. Signal integrals afforded the concentrations of **4**, **5**, ATP, ADP, CTP, and pyrophosphate in the equilibrium mixture.

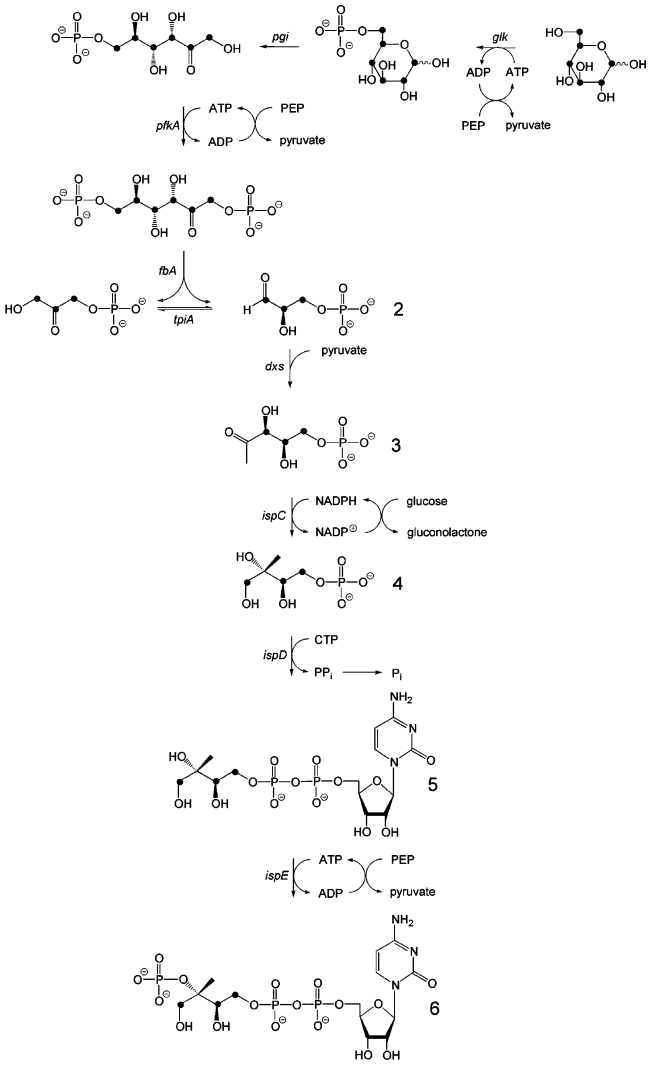

FIGURE 2. Synthesis of [1,3,4-^{13}C$_3$]4-diphosphocytidyl-2*C*-methyl-D-erythritol 2-phosphate (**6**) from [U-^{13}C$_6$]glucose. ^{13}C-atoms are indicated by full circles.

The equilibrium substrate and product concentrations in reaction mixtures containing large amounts of enzymes could also be monitored by ^{13}C NMR spectroscopy using ^{13}C-labeled

(25) Jomaa, H.; Wiesner, J.; Sanderbrand, S.; Altincicek, B.; Weidemeyer, C.; Hintz, M.; Turbachova, I.; Eberl, M.; Zeidler, J.; Lichtenthaler, H. K.; Soldati, D.; Beck, E. *Science* **1999**, *285*, 1573−1576.
(26) Borrmann, S.; Issifou, S.; Esser, G.; Adegnika, A. A.; Ramharter, M.; Matsiegui, P. B.; Oyakhirome, S.; Mawili-Mboumba, D. P.; Missinou, M. A.; Kun, J. F.; Jomaa, H.; Kremsner, P. G. *J. Infect. Dis.* **2004**, *190*, 1534−1540.
(27) Missinou, M. A.; Borrmann, S.; Schindler, A.; Issifou, S.; Adegnika, A. A.; Matsiegui, P. B.; Binder, R.; Lell, B.; Wiesner, J.; Baranek, T.; Jomaa, H.; Kremsner, P. G. *Lancet* **2002**, *360*, 1941−1942.
(28) Kuzuyama, T.; Shimizu, T.; Takahashi, S.; Seto, H. *Tetrahedron Lett.* **1998**, *39*, 7913−7916.
(29) Bernal, C.; Palacin, C.; Boronat, A.; Imperial, S. *Anal. Biochem.* **2005**, *337*, 55−61.
(30) Bernal, C.; Mendez, E.; Terencio, J.; Boronat, A.; Imperial, S. *Anal. Biochem.* **2005**, *340*, 245−251.
(31) Kuzuyama, T.; Takahashi, S.; Takagi, M.; Seto, H. *J. Biol. Chem.* **2000**, *275*, 19928−19932.
(32) Hecht, S.; Kis, K.; Eisenreich, W.; Amslinger, S.; Wungsintaweekul, J.; Herz, S.; Rohdich, F.; Bacher, A. *J. Org. Chem.* **2001**, *66*, 3948−3952.
(33) Taylor, S. V.; Long, V. D.; Begley, T. P.; Schoerken, U.; Grolle, S.; Sprenger, G. A.; Bringer-Meyer, S.; Sahm, H. *J. Org. Chem.* **1998**, *63*, 2375−2377.
(34) Blagg, B. S. J.; Poulter, C. D. *J. Org. Chem.* **1999**, *64*, 1508−1511.
(35) Kis, K.; Wungsintaweekul, J.; Eisenreich, W.; Zenk, M. H.; Bacher, A. *J. Org. Chem.* **2000**, *65*, 587−592.
(36) Hoeffler, J. F.; Pale-Grosdemange, C.; Rohmer, M. *Tetrahedron Lett.* **2000**, *56*, 1485−1489.
(37) Koppisch, A. T.; Blagg, B. S.; Poulter, C. D. *Org. Lett.* **2000**, *2*, 215−217.
(38) Fontana, A. *J. Org. Chem.* **2001**, *66*, 2506−2508.
(39) Hecht, S.; Wungsintaweekul, J.; Rohdich, F.; Kis, K.; Radykewicz, T.; Schuhr, C. A.; Eisenreich, W.; Richter, G.; Bacher, A. *J. Org. Chem.* **2001**, *66*, 7770−7775.
(40) Rohdich, F.; Schuhr, C. A.; Hecht, S.; Herz, S.; Wungsintaweekul, J.; Eisenreich, W.; Zenk, M. H.; Bacher, A. *J. Am. Chem. Soc.* **2000**, *122*, 9571−9594.
(41) Schuhr, C. A.; Hecht, S.; Kis, K.; Eisenreich, W.; Wungsintaweekul, J.; Bacher, A.; Rohdich, F. *Eur. J. Org. Chem.* **2001**, *17*, 3221−3226.
(42) Giner, J. L.; Ferris, W. V., Jr. *Org. Lett.* **2002**, *4*, 1225−1226.
(43) Amslinger, S.; Kis, K.; Hecht, S.; Adam, P.; Rohdich, F.; Arigoni, D.; Bacher, A.; Eisenreich, W. *J. Org. Chem.* **2002**, *67*, 4590−4594.
(44) Ward, J. L.; Beale, M. H. *J. Chem. Soc., Perkin Trans.* **2002**, *I*, 710−712.

TABLE 1. ^{31}P NMR Data of the Reactants Used

position	chemical shifts ppm[a]	coupling constants, Hz J_{PP}	J_{PC}[b]
ADP	−5.29 (d)	22.3	
	−9.48 (d)	22.3	
ATP	−5.21 (d)	19.6	
	nd[c]	nd[c]	
	−20.73 (t)	19.6	
CTP	−4.38 (d)	15.6	
	−9.36 (d)	15.6	
	−17.98 (t)	15.6	
pyrophosphate	−4.3 (s)		
4	5.33 (dd)		4.9, 6.2
5	−9.47 (ddd)	20.9	7.6, 5.8
	−10.08 (d)	20.9	

[a] Referenced to external 85% H_3PO_4. Signal multiplicities are given in the parentheses. [b] Observed with [1,3,4-$^{13}C_3$]-**4** or -**5**, respectively. [c] Not determined due to signal overlap.

TABLE 2. ^{13}C NMR Data of the Reactants Used

position	chemical shift ppm ^{13}C[a]	coupling constant, Hz J_{CC}	J_{PC}
[3,4,5-$^{13}C_3$]1-deoxy-D-xylulose 5-phosphate (**3**)			
3	77.1	39.6	
4	70.8	39.6, 43.6	6.8
5	64.2	43.6	4.6
[1,3,4-$^{13}C_3$]2*C*-methyl-D-erythritol 4-phosphate (**4**)			
1	66.5		
3	73.8	42.2	6.4
4	64.9	42.2	4.2
[1,3,4-$^{13}C_3$]4-diphosphocytidyl-2*C*-methyl-D-erythritol (**5**)			
1	66.4		
3	73.4	42.7	7.5
4	67.1	42.7	5.5
[1,3,4-$^{13}C_3$]4-diphosphocytidyl-2*C*-methyl-D-erythritol 2-phosphate (**6**)			
1	65.9		2.0, 1.8
3	74.0	42.9	7.1, 7.1
4	67.2	42.9	5.8

[a] Referenced to external trimethylsilylpropane sulfonate.

substrates (Table 2). In good agreement, the different measurement methods afford an equilibrium constant (calculated from eq 1) of 0.38 for the reaction catalyzed by IspD protein at pH 8.0 and 37 °C.

$$K = \frac{[5][PP_i]}{[4][CTP]} \quad (1)$$

In a similar approach, we showed that the equilibrium constant (as defined by eq 2) for the reaction catalyzed by IspE protein is 6.5 at pH 8.0 and 37 °C. Notably, we confirmed that the equilibrium can be reached using either **5** or **6** as starting material; hence, there can be no doubt that the reaction shows full reversibility under our experimental conditions and was not limited by insufficient enzyme activity.

$$K = \frac{[6][ADP]}{[5][ATP]} \quad (2)$$

To obtain a high yield of 4-diphosphocytidyl-2*C*-methyl-D-erythritol 2-phosphate (**6**) (Figure 2), it was mandatory, in light

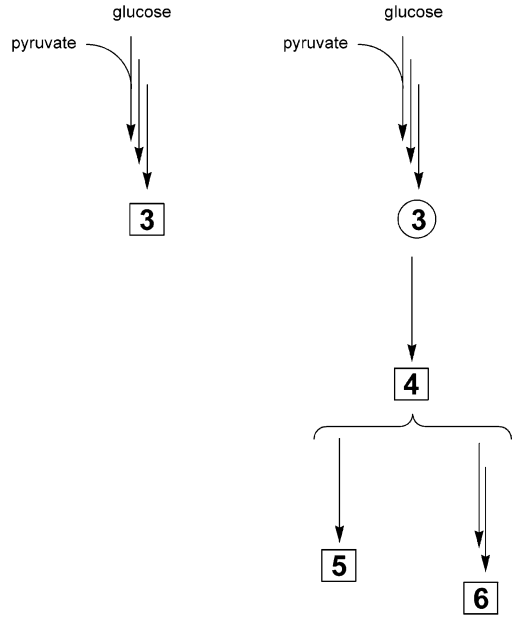

FIGURE 3. Flux diagram for synthesis and isolation procedures of nonmevalonate isoprenoid pathway intermediates. Symbols: ○, removal of protein by ultrafiltration; □, product purification.

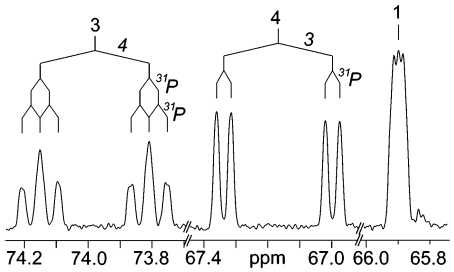

FIGURE 4. ^{13}C NMR signals of [1,3,4-$^{13}C_3$]4-diphosphocytidyl-2*C*-methyl-D-erythritol 2-phosphate (**6**). Coupling patterns are indicated.

of the equilibrium constants, to drive the reaction in the forward direction by coupled exergonic processes. For this purpose, we included inorganic pyrophosphatase into the reaction mixture in order to degrade pyrophosphate, the second product of the reaction catalyzed by IspD protein. Moreover, we implemented a regeneration system for ATP comprising pyruvate kinase and phosphoenol pyruvate in order to maximize the free energy gradient of the phosphorylation reaction catalyzed by IspE protein; that approach had the additional advantage that ATP is only required in catalytic amounts, thus facilitating the chromatographic purification of the product.

In earlier work,[41] we had shown that 2*C*-methyl-D-erythritol 2,4-cyclodiphosphate (**7**) can be obtained in a one-pot reaction from glucose. In principle, a similar approach should be possible for 4-diphosphocytidyl-2*C*-methyl-D-erythritol 2-phosphate (**6**). However, since we found that **6** is not easily separated from reagents used in its preparation, we decided to produce and

(45) Wolff, M.; Seemann, M.; Grosdemange-Billiard, C.; Tritsch, D.; Campos, N.; Rodriguez-Concepción, M.; Boronat, A.; Rohmer, M. *Tetrahedron Lett.* **2002**, *43*, 2555−2559.
(46) Fox, D. T.; Poulter, C. D. *J. Org. Chem.* **2002**, *67*, 5009−5010.
(47) Gao, W.; Loeser, R.; Raschke, M.; Dessoy, M. A.; Fulhorst, M.; Alpermann, H.; Wessjohann, L. A.; Zenk, M. H. *Angew. Chem., Int. Ed.* **2002**, *41*, 2604−2607.
(48) Giner, J. L. *Tetrahedron Lett.* **2002**, *43*, 5457−5459.
(49) Hecht, S.; Amslinger, S.; Jauch; Kis, K.; Trentinaglia, V.; Adam, P.; Eisenreich, W.; Bacher, A.; Rohdich, F. *Tetrahedron Lett.* **2002**, *43*, 8929−8933.

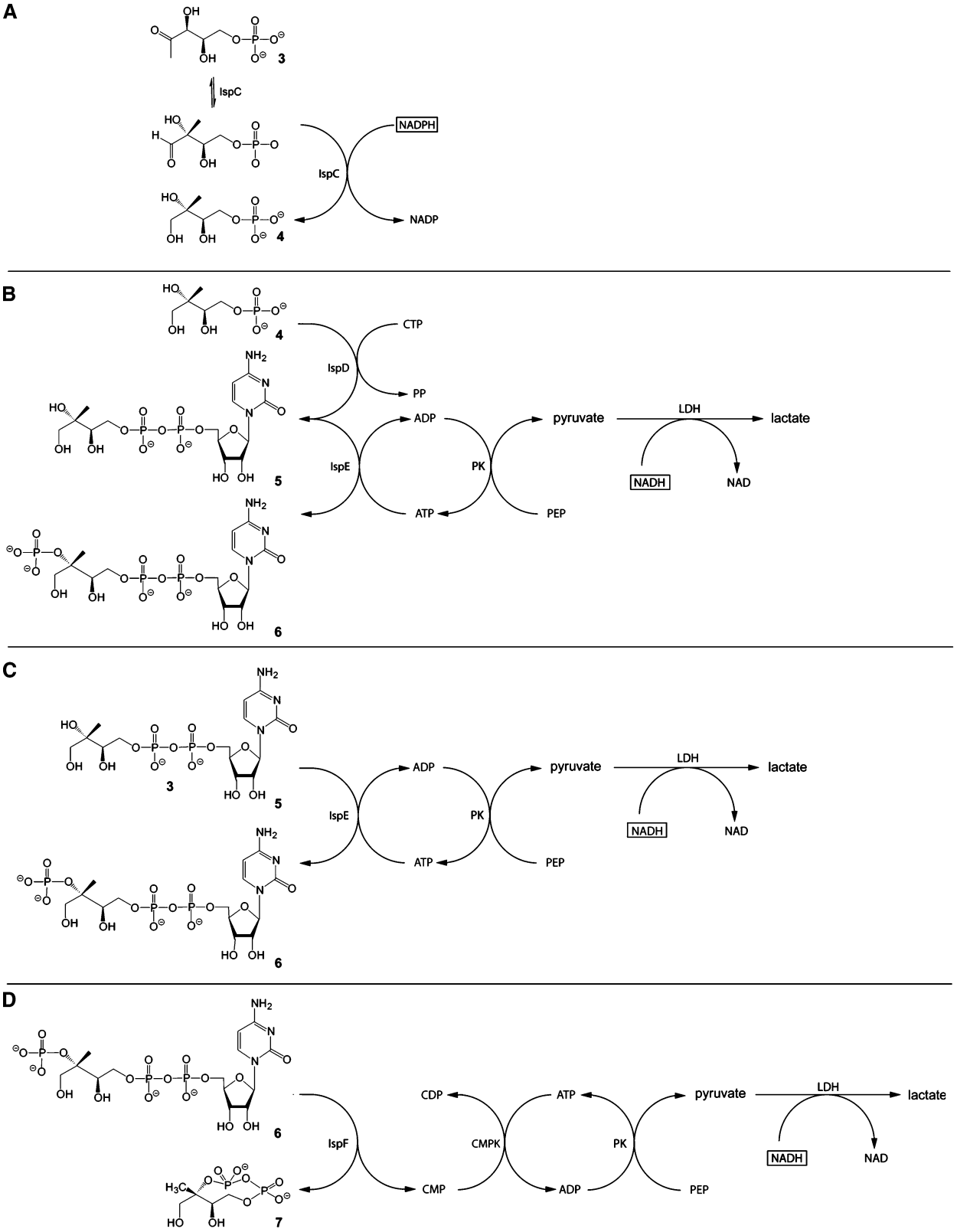

FIGURE 5. High-throughput screening assays for IspC (A), IspD (B), IspE (C), and IspF (D) proteins.

purify 2*C*-methyl-D-erythritol 4-phosphate (**4**) which can then be converted into **6** by a one-pot reaction (Figure 3).

With the use of ^{13}C-labeled **4** (prepared from ^{13}C-labeled glucose), the formation of **6** can be followed conveniently by ^{13}C NMR analysis. With the use of the hydrolysis of inorganic pyrophosphate and phosphoenol pyruvate as the driving forces for the overall reaction, the conversion of **4** into **6** can be brought virtually to completion as diagnosed by NMR detection of ^{13}C-coupled reactant species. Under the experimental conditions described, the reaction requires about 3 h. The product **6** can be purified by column chromatography on Whatman cellulose using isocratic elution. The yield of **6** based on **4** is 50%. The

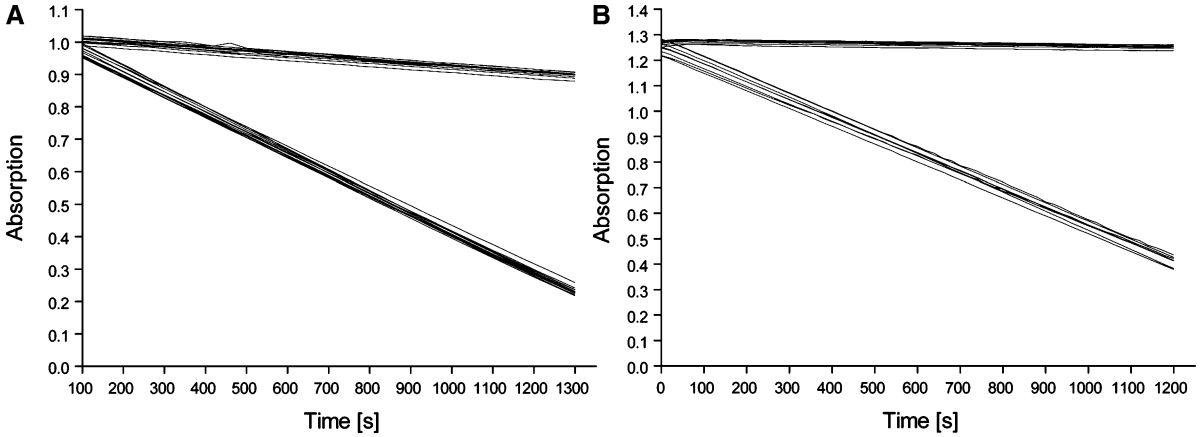

FIGURE 6. Absorbance vs time 96-well plate photometric assays of the IspD (A) and IspE (B) reaction. (A) Twelve control assays without and 12 signal assays with substrate (**4**); (B) 8 control assays without and 8 signal assays with substrate (**5**).

overall yield of **6** based on ^{13}C-labeled glucose serving as starting material is 40%. The effective yield is mainly determined by losses during column chromatography workup but is still high if one takes into account that the conversion of glucose into **6** involves nine reaction steps.

The present strategy enables the incorporation of stable isotopes as well as radioisotopes into various positions of **6**. Notably, ^{13}C can be incorporated into virtually any position of the polyol moiety from appropriately labeled glucose and/or pyruvate as starting material. Numerous isotopologs of glucose and of pyruvate are commercially available, and single-labeled as well as multiply labeled isotopologs of **6** can be prepared as required.

We have used this enzyme-assisted synthesis to prepare multigram amounts of **6** as required to screen large compound libraries for inhibitors of IspF protein. Figure 4 shows the ^{13}C NMR signature of [1,3,4-$^{13}C_3$]-**6** obtained by this method.

The procedures described in the Experimental Section also provide improved technology for the preparation of large amounts (multigram scale) of **4**. Specifically, the improved procedure affords a yield of 80% ^{13}C-labeled **4** based on ^{13}C-labeled glucose, as compared to about 50% reported for our previously published method.[39] Moreover, we report an improved workup procedure for the isolation of **3** which can now be prepared with a yield of about 85% based on ^{13}C-labeled glucose.

An improved procedure for the preparation of **5**[40] is also reported. The modified method uses inorganic pyrophosphatase in order to drive the reaction forward. This is advantageous in order to counteract the impact of the relatively unfavorable equilibrium constant of the reaction catalyzed by IspD protein. Whereas the reported two-step procedure is similar in terms of overall yield (based on ^{13}C-labeled glucose) as compared to the procedure reported earlier, the present procedure does not require preparative HPLC purification of the product (notably, the earlier procedure involved two consecutive HPLC purification steps) and can be easily applied for the preparation of multigram amounts. Scale-up to even larger bulk quantities would be possible without significant further modification.

Improved yields and/or purity of the synthetic compounds reported in this paper are in part due to improved quality of the proteins used for multicomponent enzyme-assisted synthesis. Whereas we have previously used auxiliary enzymes from commercial sources, we have now introduced several recombinant enzymes (fructose 1,6-biphosphate aldolase, phosphofructokinase, and glucose 6-phosphate isomerase) which can be obtained in highly purified form by affinity chromatography. This modification of the technology was driven by the observation that commercial preparations may contain significant amounts of contaminating enzyme activities that reroute intermediates to undesired side products. This can become precarious in multicomponent/multicatalyst reaction mixtures.

TABLE 3. ***Z*-Factors for the High-Throughput Screening Assays of the IspC, IspD, IspE, and IspF Reactions**

assay	*Z*-factor
IspC	0.88
IspD	0.92
IspE	0.89
IspF	0.86

High-Throughput Assays. The reaction schemes used in the present study are summarized in Figure 5. Whereas the reaction catalyzed by IspC protein is inherently chromogenic (via the consumption of NADPH; Figure 5A), the reactions catalyzed by the IspDEF enzymes[22] need to be coupled to appropriate chromogenic reactions in order to enable photometric monitoring in the near-UV range.

IspE protein uses ATP as a second substrate. ATP consumed by the reaction under formation of ADP can be regenerated by pyruvate kinase using phosphoenol pyruvate as substrate. The resulting pyruvate can be converted into lactate by lactate dehydrogenase. The consumption of NADH by that reaction can be monitored at 340 nm (Figure 5C).

The formation of pyruvate from phosphoenol pyruvate is highly exergonic, especially when pyruvate is continuously removed by reduction affording lactate. Thus, the auxiliary enzymes used in the assay lock the ATP/ADP ratio at a high value. The resulting quasi-steady concentration of ATP simplifies the kinetic algorithm describing the IspE-catalyzed reaction in two different ways. (i) The forward reaction rate becomes apparently independent of the ATP concentration. (ii) The backward reaction is virtually suppressed, since the cosubstrate, ADP, is only present at a low concentration; this is especially important in light of the unfavorable equilibrium constant of the IspE-catalyzed reaction.

The topology of the assay for IspD protein shown in Figure 5B is similar to that used for IspE protein. Specifically, the product of IspD protein, **5**, is converted into **6** by IspE enzyme,

and that reaction is then monitored via pyruvate kinase and lactate dehydrogenase. As in the previous case, the Gibbs free energy gradient of the hydrolysis of phosphoenol pyruvate is used to make the reaction of IspD protein essentially irreversible.

The IspF assay shown in Figure 5D is based on the conversion of cytidyl phosphate (CMP), the second product of the IspF-catalyzed reaction, into CDP by cytidylate kinase (CMP kinase) using ATP as substrate. ATP is regenerated from the resulting ADP by pyruvate kinase using phosphoenol pyruvate as substrate. The resulting pyruvate is converted to lactate by lactate dehydrogenase using NADH as cosubstrate. The production of NAD^+ is again monitored photometrically at 340 nm. As in the previous cases, the Gibbs free energy gradient of pyruvate formation is used to drive the IspF reaction in the forward direction.

For the multicomponent assays used for the IspDEF proteins, it is crucial that the index reaction should be the bottleneck of the entire reaction sequence. To achieve that, the overall catalytic rate of the auxiliary enzyme cascade must be made large enough as compared to the catalytic rate of the enzyme catalyzing the primary reaction. In the present case, the auxiliary enzymes are used in amounts that ensure a 100-fold excess of enzymatic activity as compared to the index enzyme. More specifically, the reaction conditions have been adjusted for the consumption of NADH to proceed with a linear progression rate until at least 30% of the substrate is consumed (Figure 6).

All reactions shown in Figure 6 were implemented on a plate reader (96-well format). With the use of that experimental setup, *Z*-factors (cf., Table 3) for all high-throughput assays reported in this paper were calculated from eq 3

$$Z = 1 - \frac{(3\sigma_s + 3\sigma_c)}{|\mu_s - \mu_c|} \quad (3)$$

where σ is the standard deviation, μ the mean value, s the signal, and c the control.[50] As shown in Table 3, they are all ≥ 0.86. Generally, assays with *Z*-factors above 0.5 are considered as sufficiently robust for the screening of large libraries.[50]

Assay Methods for Hit Verification. For all screening methods described above, it is essential to verify potential hits by an independent analytical method. For that purpose, we developed assays monitored by ^{13}C NMR spectroscopy, which were designed specifically for direct assessment of the specific enzyme product rather than a coenzyme or surrogate reactant. The reported methods for the preparation of enzyme substrates are all perfectly suited to prepare a variety of ^{13}C-labeled isotopologues from commercially available isotopologues of glucose. With the use of ^{13}C-labeled substrates, the sensitivity of ^{13}C NMR monitoring is increased by 2 orders of magnitude as compared with assays using unlabeled substrate. Moreover, the selectivity of these assays is high due to the relatively large chemical shift range for ^{13}C which results in excellent resolution of the signals of substrates, products, and potential side products. Maximum selectivity, at the cost of slightly reduced sensitivity, can be achieved by multiple ^{13}C-labeling. In that case, each reaction component is reflected in the NMR spectrum by several high-intensity signals representing all labeled carbon atoms; moreover, the specific $^{13}C^{13}C$ coupling constants can serve as additional compound identifiers (Figure 7). ^{13}C NMR signatures

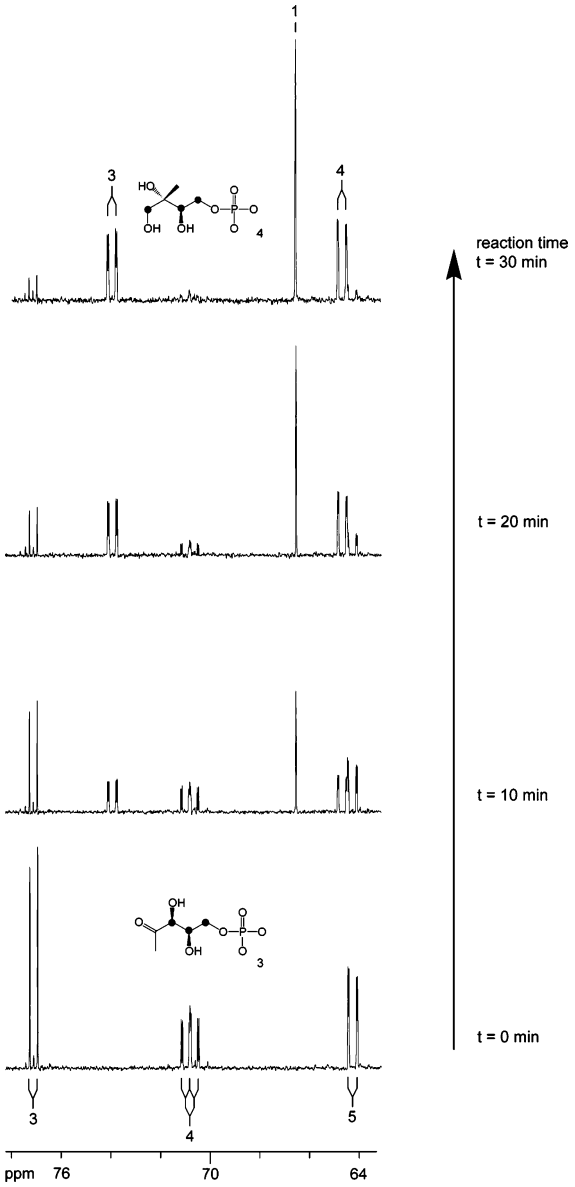

FIGURE 7. NMR assay of the IspC reaction for hit follow-up. The signal height was normalized using uniformly ^{13}C-labeled acetate as the standard.

of [1,3,4-$^{13}C_3$]-**4**, [1,3,4-$^{13}C_3$]-**5**, and [1,3,4-$^{13}C_3$]-**6** that can all be prepared from [U-$^{13}C_6$]glucose are summarized in Table 2.

For all Isp proteins in the present study, we have shown that the rates obtained by the optical multicomponent assay and the NMR assay agree within close limits. Using a relatively high concentration of the ^{13}C-labeled substrate, we observed quasi-linear progression curves over a relatively wide range of reaction progression.

Discussion

Computer-controlled devices for monitoring very large numbers of enzyme assays and other bioassays are now widely distributed and have substantially changed the process of lead compound discovery. Typical assay formats employ microtiter plates with 96 or 384 wells that can be monitored by a variety of optical methods. The selection of the format is characterized by a tradeoff between reaction volume and, hence, consumption

(50) Zhang, J. H.; Chung, T. D.; Oldenburg, K. R. *J. Biomol. Screen* **1999**, *4*, 67−73.

of reagents, on one side and robustness of the assay on the other side. However, it must be emphasized that the screening of large libraries comprising tens of thousands or even hundreds of thousands of compounds continues to require substrates and proteins in relatively large amounts (upper milligram to multigram range). To give a specific example, the screening of a 100 000 compound library against IspF protein in the 384-well format with absorbance monitoring requires about 2.5 g of substrate (**6**), 2 g of NADH, 6.6 g of ATP, 3.1 g of phosphoenol pyruvate, 100 mg of target protein (IspF protein), 2 g of CMP kinase, and 33 000 U of pyruvate kinase and lactate dehydrogenase each as auxiliary enzymes. The successful high-throughput implementation of a given assay therefore depends crucially on methodology for the preparation of target proteins, substrates, and required auxiliary enzymes at acceptable cost and effort unless the reagents are commercially available in relatively large quantities at acceptable costs.

The present study was conducted with the aim to provide a robust platform for four enzymes of the nonmevalonate pathway. All aspects of the production of enzymes and enzymes in quantities sufficient for screening libraries (in the 100 000 compound range) are covered in this presentation. More specifically, the authors have actually prepared all these required reagents in sufficient amounts for the screening of 100 000 compound libraries in the course of this study; notably, this was done in a standard research laboratory setting without the use of larger facilities. Although the reported biochemical preparations were performed in several consecutive batches, the work comprises no hidden scale-up factors that would have to be taken into account in order to procure sufficient material for the screening of large libraries.

The actual production of these large reagent amounts depended crucially on affinity purification of highly expressed recombinant enzymes that were used as target proteins, auxiliary proteins, and/or catalysts for substrate production. It should also be noted that we describe a pipeline for the enzyme-assisted production of all required enzyme substrates. That pipeline requires only glucose and pyruvate as specific substrates. ATP and pyridine nucleotides are the only required coenzymes. For all required enzymes of the nonmevalonate pathway, we provide laboratory-scale technology that enables the preparation of the gram or multigram amounts required. Since we have found that our multistep enzyme procedures are to some extent compromised by spurious enzyme activities in commercially available enzymes, we also report technology for the production of auxiliary enzymes (fructose 1,6-bisphosphate aldolase, phosphofructokinase, glucose 6-phosphate isomerase, and CMP kinase) in recombinant form by highly efficient and standardized affinity chromatography (nickel-chelating) columns.

The multienzyme cascade for the preparation of early nonmevalonate intermediates (from glucose and pyruvate as substrates by one-pot strategies without intermediate isolation) can be exited at the level of **3** or **4** (as described in more detail in this paper) or at the level of **5** as described in an earlier paper. Notably, the multistep procedure involves the removal of enzymes by ultrafiltration after the formation of **3** is complete, but conversion of **3** to **4**, if required, is performed by addition of additional reagents to the ultrafiltrate and continued incubation of that mixture, without isolation of intermediate **3**. Since various isotopologs of both starting materials are commercially available, virtually every desired product isotopologue can be obtained without modification of the experimental technique (except the use of differently labeled starting materials).

By comparison with our previous reports, we now report significantly improved yields, in the range of 80% based on substrate glucose, for the preparation of **3** and **4**. These improved yields are mainly due to the use of affinity-purified auxiliary enzymes (fructose 1,6-bisphosphate aldolase, phosphofructokinase, glucose 6-phosphate isomerase) instead of commercial products and to improved chromatography procedures that have the additional advantage that they could be easily scaled up to larger batches than those reported in the present paper in case that the need should arise.

With a starting material as cheap as glucose, an increase of the conversion yield from about 50%[39] to about 80% would appear to be devoid of practical significance although it would continue to be of academic interest in view of seven reaction steps from glucose to **4** (notably, the overall yield of 80% translates into an average yield of about 97% per reaction step). More importantly, however, the aspect of improved yields translates into a substantial advantage when ^{13}C-labeled glucose is used as substrate. It should also be noted that the increased yields implicate reduced formation of undesired side products, and that translates into facilitated purification and improved product purity.

Whereas we have previously reported one-pot procedures for the preparation of **5** and **7** starting with glucose and pyruvate as substrates, we found a two-stage method with isolation and purification of intermediate **4** preferable for the preparation of **6**. This tactical change became necessary in order to enable a robust method for product purification by column chromatography on fibrous cellulose that can be scaled beyond the millimole level at acceptable costs and without loss of resolution.

In the wake of that development, we also decided to reconfigure the preparation of **5** as a two-stage procedure with isolation and purification of intermediate **4**. The product of the two-stage reaction sequence can be obtained in pure form by chromatography on conventional cellulose columns, whereas the one-pot strategy reported earlier had required two sequential steps of preparative HPLC purification. Whereas the overall yield of the novel procedure is not improved by comparison with the older one-pot procedure, the overall effort is lower. Notably, the enzymatic conversion of **4** into **5** and **6**, respectively, is essentially quantitative as can be documented easily when the reaction is conducted with ^{13}C-labeled **4** and is monitored by ^{13}C NMR. However, the technically simple purification on conventional cellulose columns comes at the price of yield deterioration.

The high-throughput assay methods described in the present study are all monitored photometrically at 340 nm. They are all based on the consumption of a reduced pyrimidine nucleotide. We are aware that enhanced sensitivity and, consequently, a reduced requirement for reagents, would be possible by fluorescence readout, albeit at the price of reduced selectivity since fluorescence can be modulated easily by chemical quenching, and many compounds in typical compound libraries are effective quenchers. Whereas test compounds may also have absorbance at 340 nm, that is a minor concern since those contributions are detected by the absorbance measurement at the start of the reaction.

Notably, our high-throughput assays have all been implemented on an automatic plate reader for 96-well plates where they had *Z*-factors of 0.86 or better. In the literature, assays

with *Z*-factors above 0.5 are generally considered as robust. The assays reported in this paper are well above that limit.

As already mentioned in the Introduction, assay methods that can be monitored photometrically have been reported by other authors for IspC, IspD, and IspE.[29−31] For IspD protein, Boronat and co-workers used an end point assay based on the detection of inorganic pyrophosphate generated by IspD protein. More specifically, they converted inorganic pyrophosphate into orthophosphate that was complexed with the dye malachite green, and that complex was detected at 630 nm. The IspE reaction was monitored by Boronat and co-workers by rephosphorylation of ADP and reduction of the resulting pyruvate under consumption of NADH according to Figure 5C; independently, the same strategy had been developed by our research group, prior to the publication of Boronat et al. A high-throughput assay for IspC protein based on thermodynamic rather than catalytic principles has been established and used by Gottlin et al.[51] That assay is based on binding of the protein to a solid-phase bound surrogate substrate.

Even highly robust high-throughput assays will generate a certain amount of false positives. In the present case, the use of auxiliary enzymes could select for compounds that inhibit one of the enzymes in the auxiliary cascade rather than the target enzyme. To minimize the chance of such an event, the assays reported in this paper use the auxiliary enzymes in large excess (as defined in terms of catalytic power) over the target enzyme. Thus, only very strong inhibitors of auxiliary enzymes would result in false positives. The use of auxiliary enzymes in large excess over the target enzyme has the additional advantage that the apparent reaction rate is an almost accurate representation of the catalytic rate of the index enzyme which has been made the bottleneck of the entire reaction sequence. As an additional advantage of that strategy, the progression curves of all assays reported in this paper are linear over a range of at least 30% of substrate consumption (cf., Figure 6); this simplifies data interpretation quite considerably.

With all these safeguards in place, it is still highly desirable to monitor the reaction by a completely independent strategy. Again with the aim to provide a uniform assay platform for all four enzymes under study, we report a set of assays where product formation by the index enzyme is directly monitored by ^{13}C NMR spectroscopy using singly or multiply ^{13}C-labeled substrates which can be prepared as described above. These assays combine relatively high sensitivity (due to >99% ^{13}C enrichment of the analyte) with extraordinary selectivity due to the large chemical shift range of ^{13}C. Notably, that selectivity can be further enhanced by multiple labeling which is conducive to the observations of extremely characteristic multiplet signatures for the ^{13}C-labeled molecular positions (cf., Figure 7).

During the relatively short time that has elapsed since the elucidation of the nonmevalonate pathway, orthologs of the IspCDEF enzymes have been obtained in recombinant form from a variety of pathogenic organisms including IspC protein from *M. tuberculosis*[52] and *P. falciparum*,[25] IspDF from *Campylobacter jejuni*,[53] and IspF from *P. falciparum*.[54] Three-dimensional structures are also available for each of these enzymes, typically for different orthologs.[55−58] In addition to that, the present paper provides a coherent set of methods for the preparation of all required enzyme substrates in multigram amounts, in high purity, with or without ^{13}C-labeling. All assays use pyridine nucleotide biochemistry for rate measurements, and their robustness has been checked rigorously and has been shown to be sufficient for the screening of large libraries. Rigorous tests for hit verification by NMR spectroscopy are also reported. This integrated concept is available for antiinfective drug screening without any requirement for additional method development and standardization.

Experimental Section

A. Construction of a Recombinant Strain for Hyperexpression of the *E. coli fbA, pfkA, pgi,* and *cmpK* Genes. The *fbA*, *pfkA*, *pgi*, and *cmpK* genes of *E. coli* coding for fructose 1,6-bisphosphate aldolase, phosphofructokinase, glucose 6-phosphate isomerase, and CMP kinase (accession no. gb U00096.2) were amplified by PCR using chromosomal *E. coli* DNA as the template and the oligonucleotides shown in the Supporting Information as the primers. The amplificates were digested with restriction endonucleases (see the Supporting Information), and the resulting fragments were ligated into the expression vector pQE30 which had been digested with the same restriction enzymes. The ligation mixtures were electroporated into *E. coli* XL1-Blue[59] and M15 [pREP4][60] cells (see the Supporting Information).

B. Sequence Determination. DNA sequencing was performed by the automated dideoxynucleotide method. N-terminal peptide sequences were obtained by the pulsed-liquid mode.

C. Culturing Recombinant Bacteria. Recombinant *E. coli* strains were grown in Luria Bertani broth containing ampicillin (180 mg L^{-1}) and kanamycin (50 mg L^{-1}) as appropriate. Cultures were incubated at 37 °C with shaking. At an optical density of 0.7 (600 nm), isopropylthiogalactoside was added to a final concentration of 2 mM, and the cultures were incubated for 5 h. The cells were harvested by centrifugation, washed with 0.9% (w/v) sodium chloride, and stored at −20 °C.

D. Preparation of Recombinant Proteins (FbA, PfkA, Pgi, CmpK). Frozen cell mass (25 g) of the recombinant *E. coli* strains M15-pQEfbA, M15-pQEpfkA, M15-pQEpgi, and M15-pQEcmp*K*, respectively, was thawed in 120 mL of 100 mM Tris hydrochloride, pH 8.0, containing 0.5 M sodium chloride and 20 mM imidazole hydrochloride. The cells were disrupted by treatment with a French press, and the suspension was centrifuged. The supernatant was applied to a column of Ni^{2+}-chelating Sepharose FF (column volume, 20 mL) which had been equilibrated with 100 mM Tris hydrochloride, pH 8.0, containing 0.5 M sodium chloride and 20 mM imidazole (flow rate, 2 mL/min). The column was washed with 100 mL of 100 mM Tris hydrochloride, pH 8.0, containing 0.5 M sodium chloride and 20 mM imidazole and was then developed with a gradient of 20−500 mM imidazole in 100 mM Tris hydrochloride, pH 8.0, containing 0.5 M sodium chloride (total

(51) Gottlin, E. B.; Benson, R. E.; Conary, S.; Antonio, B.; Duke, K.; Payne, E. S.; Ashraf, S. S.; Christensen, D. J. *J. Biomol. Screening* **2003**, *8*, 332−339.
(52) Argyrou, A.; Blanchard, J. S. *Biochemistry* **2004**, *43*, 4375−4384.
(53) Gabrielsen, M.; Rohdich, F.; Eisenreich, W.; Gräwert, T.; Hecht, S.; Bacher, A.; Hunter, W. N. *Eur. J. Biochem.* **2004**, *271*, 3028−3035.
(54) Rohdich, F.; Eisenreich, W.; Wungsintaweekul, J.; Hecht, S.; Schuhr, C. A.; Bacher, A. *Eur. J. Biochem.* **2001**, *268*, 3190−3197.
(55) Steinbacher, S.; Kaiser, J.; Eisenreich, W.; Huber, R.; Bacher, A.; Rohdich, F. *J. Biol. Chem.* **2003**, *278*, 18401−18407.
(56) Richard, S. B.; Bowman, M. E.; Kwiatkowski, W.; Kang, I.; Chow, C.; Lillo, A. M.; Cane, D. E.; Noel, J. P. *Nat. Struct. Biol.* **2001**, *8*, 641−648.
(57) Miallau, L.; Alphey, M. S.; Kemp, L. E.; Leonard, G. A.; McSweeney, S. M.; Hecht, S.; Bacher, A.; Eisenreich, W.; Rohdich, F.; Hunter, W. N. *Proc. Natl. Acad. Sci. U.S.A.* **2003**, *100*, 9173−9178.
(58) Steinbacher, S.; Kaiser, J.; Wungsintaweekul, J.; Hecht, S.; Eisenreich, W.; Gerhardt, S.; Bacher, A.; Rohdich, F. *J. Mol. Biol.* **2002**, *316*, 79−88.
(59) Bullock, W. O.; Fernandez, J. M.; Short, J. M. *Biotechniques* **1987**, *5*, 376−379.
(60) Zamenhof, P. J.; Villarejo, M. *J. Bacteriol.* **1972**, *110*, 171−178.

volume, 100 mL). Fractions were combined and dialyzed overnight against 100 mM Tris hydrochloride, pH 8.0, and stored at −80 °C.

E. Preparation of [3,4,5-$^{13}C_3$]1-Deoxy-D-xylulose 5-Phosphate (3). [3,4,5-$^{13}C_3$]-**3** was prepared according to published procedures[32] with modifications as described below. A reaction mixture containing 150 mM Tris hydrochloride, 10 mM magnesium chloride, 1 g (4.9 mmol) of [U-$^{13}C_6$]glucose, 0.099 g (0.18 mmol) of ATP, 0.23 g (1.5 mmol) of dithiothreitol, 0.3 g (0.65 mmol) of thiamine diphosphate, and 2.2 g (10.6 mmol) of potassium phosphoenol pyruvate in a total volume of 300 mL was adjusted to pH 8.0 by the addition of 5 M sodium hydroxide. To this mixture, 9 mg (750 U) of hexokinase, 1.1 mg (570 U) of glucose 6-phosphate isomerase, 13 mg (50 U) of fructose 6-phosphate kinase, 0.1 mg (620 U) of triose phosphate isomerase, 18 mg (60 U) of fructose 1,6-biphosphate aldolase, 1.7 mg (590 U) of pyruvate kinase, and 12 mg (30 U) of 1-deoxy-D-xylulose 5-phosphate synthase (Dxs protein) were added. The final volume was 320 mL. The mixture was incubated at 37 °C. Aliquots of 50 μL were retrieved at 1 h intervals; D_2O was added to a final volume of 500 μL, and ^{13}C NMR spectra were obtained in order to monitor the reaction progress. The reaction was found to be virtually complete after 3 h. The mixture was passed through a 10 kDa ultrafiltration membrane. The solution was lyophilized (dry weight, 16 g).

Aliquots (8 g) of the crude product were dissolved in 40 mL of 2-propanol/methanol/water (4:2:4, v/v) and purified as described below. The solution was placed on a column of microcrystalline cellulose (4 × 60 cm) which had been equilibrated with 1.8 L of 2-propanol/methanol/H_2O (4:2:4, v/v). The column was then developed with 2 L of 2-propanol/methanol/H_2O (4:2:4, v/v) (flow rate, 1.5 mL/min). Fractions were collected and analyzed using cellulose TLC plates which were developed with a mixture of 2-propanol/methanol/water (4:2:4, v/v), dried, sprayed with a mixture of acetic acid/sulfuric acid/anisaldehyde (100:1:2, v/v),[61] and heated at 110 °C. The product afforded violet spots (R_f value = 0.7). Fractions were combined and evaporated to a volume of about 100 mL under reduced pressure. The solution was lyophilized affording [3,4,5-$^{13}C_3$]-**3** as a white powder with an overall yield of about 85%. The concentration of [3,4,5-$^{13}C_3$]-**3** was determined by ^{13}C NMR using [1-$^{13}C_1$]glucose as an internal standard.

F. Preparation of [1,3,4-$^{13}C_3$]2*C*-Methyl-D-erythritol 4-Phosphate (4). To a solution of [3,4,5-$^{13}C_3$]-**3** (solution of crude product after removal of enzymes by ultrafiltration, 300 mL, see above), 2.25 g (11 mmol) of glucose (unlabeled), 250 mg (300 mmol) of $NADP^+$, 1.4 mg (150 U) of glucose dehydrogenase, and 24 mg (100 U) of IspC protein were added (final volume, 300 mL), and the mixture was incubated at 37 °C. The formation of [1,3,4-$^{13}C_3$]-**4** was monitored by ^{13}C NMR and was found to be virtually complete after 3 h. The mixture was passed through a 10 kDa ultrafiltration membrane and lyophilized (dry weight, 17 g). Aliquots (8.5 g) of the crude product were purified according to the procedure described for [3,4,5-$^{13}C_3$]-**3**. The procedure afforded [1,3,4-$^{13}C_3$]-**4** as a white powder with an overall yield of about 80%. The concentration of [1,3,4-$^{13}C_3$]-**4** was determined by ^{13}C NMR using [1-$^{13}C_1$]glucose as an internal standard.

G. Preparation of [1,3,4-$^{13}C_3$]4-Diphosphocytidyl-2*C*-methyl-D-erythritol (5). A reaction mixture containing 150 mM Tris hydrochloride, pH 8.0, 10 mM magnesium chloride, 0.23 g (1.5 mmol) of dithiothreitol, 2.3 g (4.3 mmol) of CTP, 4.2 mmol of [1,3,4-$^{13}C_3$]-**4**, 6 mg (50 U) of IspD protein, and 0.1 mg (100 U) of inorganic pyrophosphatase in a volume of 150 mL was incubated at 37 °C. The formation of [1,3,4-$^{13}C_3$]-**5** was monitored by ^{13}C NMR and was found to be virtually complete after 3 h.

The mixture was passed through a 10 kDa ultrafiltration membrane and lyophilized (dry weight, 7.5 g). Aliquots (1.5 g) of the crude product were dissolved in 50 mL of 2-propanol/methanol/water (4:2:4, v/v) and purified as described below. The mixture was centrifuged, and the supernatant was placed on a column of fibrous cellulose (4 × 60 cm) which had been equilibrated with 1.8 L of 2-propanol/methanol/H_2O (4:2:4, v/v). The column was then developed with 2 L of 2-propanol/methanol/H_2O (4:2:4, v/v; flow rate, 3 mL/min). The effluent was monitored photometrically at 280 nm. Fractions (25 mL) were combined and concentrated under reduced pressure to a volume of about 100 mL. The solution was lyophilized affording [1,3,4-$^{13}C_3$]-**5** as a white powder with an overall yield of about 40%. The concentration of [1,3,4-$^{13}C_3$]-**5** was determined by ^{13}C NMR using [1-$^{13}C_1$]glucose as an internal standard.

H. Preparation of [1,3,4-$^{13}C_3$]4-Diphosphocytidyl-2*C*-methyl-D-erythritol 2-Phosphate (6). A reaction mixture containing 150 mM Tris hydrochloride, pH 8.0, 10 mM magnesium chloride, 0.23 g (1.5 mmol) of dithiothreitol, 2.3 g (4.3 mmol) of CTP, 165 mg (0.3 mmol) of ATP, 1.23 g (6 mmol) of potassium phosphoenol pyruvate, 4.2 mmol of [1,3,4-$^{13}C_3$]-**4**, 6 mg (50 U) of IspD protein, 14 mg (46 U) of IspE protein, 0.8 mg (280 U) of pyruvate kinase, and 0.1 mg (100 U) of inorganic pyrophosphatase in a volume of 150 mL was incubated at 37 °C. The formation of [1,3,4-$^{13}C_3$]-**6** was monitored by ^{13}C NMR and was found to be virtually complete after 3 h.

The mixture was passed through a 10 kDa ultrafiltration membrane and lyophilized (dry weight of the residue, 7.5 g). Aliquots (1.5 g) of the crude product were purified as described above for [1,3,4-$^{13}C_3$]-**5**. The procedure affords [1,3,4-$^{13}C_3$]-**6** as a white powder with an overall yield of about 40%. The concentration of [1,3,4-$^{13}C_3$]-**6** was determined by ^{13}C NMR using [1-$^{13}C_1$]glucose as an internal standard.

I. Photometric Enzyme Assays. I.1. IspC. Assay mixtures contained 100 mM Tris hydrochloride, pH 8.0, 10 mM $MgCl_2$, 0.46 mM NADPH, 1 mM **3**, and IspC protein in a volume of 180 μL. The mixtures were incubated at 27 °C, and the reaction was monitored photometrically at 340 nm (for details of the high-throughput screen see the Supporting Information).

I.2. IspD. Assay mixtures contained 100 mM Tris hydrochloride, pH 8.0, 10 mM $MgCl_2$, 1 mM dithiothreitol, 2.5 mM potassium phosphoenol pyruvate, 2.1 mM CTP, 2 mM ATP, 1 mM **4**, 460 μM NADH, 0.4 U of IspE protein, 1 U of lactate dehydrogenase, 1 U of pyruvate kinase, and IspD protein in a volume of 180 μL. The mixtures were incubated at 27 °C, and the reaction was monitored at 340 nm (for details of the high-throughput screen see the Supporting Information).

I.3. IspE. Assay mixtures contained 100 mM Tris hydrochloride, pH 8.0, 10 mM $MgCl_2$, 2 mM dithiothreitol, 2.5 mM potassium phosphoenol pyruvate, 2 mM ATP, 1 mM **5**, 0.46 mM NADH, 1 U of lactate dehydrogenase, 1 U of pyruvate kinase, and IspE protein in a volume of 180 μL. The mixtures were incubated at 27 °C, and the absorbance was monitored at 340 nm (for details of the high-throughput screen see the Supporting Information).

I.4. IspF. Assay mixtures contained 100 mM Tris hydrochloride, pH 8.0, 10 mM $MgCl_2$, 2 mM dithiothreitol, 2.5 mM potassium phosphoenol pyruvate, 2 mM ATP, 1 mM **4**, 0.46 mM NADH, 0.5 U of CMP kinase, 1 U of lactate dehydrogenase, 1 U of pyruvate kinase, and IspF protein in a volume of 180 μL. The mixtures were incubated at 27 °C, and the absorbance was monitored at 340 nm (for details of the high-throughput screen see the Supporting Information).

J. Hit Follow-Up Assays by ^{13}C NMR. J.1. IspC. Assay mixtures contained 100 mM Tris hydrochloride, pH 8.0, 10 mM $MgCl_2$, 4 mM NADPH, 3.4 mM [3,4,5-$^{13}C_3$]-**3**, and 0.05 U of IspC protein in a volume of 500 μL. They were incubated at 27 °C, and the reaction was terminated by the addition of EDTA to a final concentration of 20 mM. D_2O was added to a final concentration of 10% (v/v). The solution was analyzed by ^{13}C NMR spectroscopy. Substrate/product ratios were obtained from the signals of C-3 of [3,4,5-$^{13}C_3$]-**3** (77.1 ppm) and C-3 of [1,3,4-$^{13}C_3$]-**4** (73.8 ppm).

(61) Jork, H.; Funk, W.; Fischer, W.; Wimmer, H. *Dünnschicht Chromatograhie: Reagenzien und Nachweismethoden*; VCH Verlagsgesellschaft: Weinheim, Basel, Cambridge, New York, 1998.

J.2. IspD. Assay mixtures contained 100 mM Tris hydrochloride, pH 8.0, 10 mM $MgCl_2$, 1 mM dithiothreitol, 4 mM CTP, 3.4 mM [1,3,4-$^{13}C_3$]-**4**, and 0.05 U of IspD protein in a volume of 500 μL. The mixtures were incubated at 27 °C, and the reaction was terminated by the addition of EDTA to a final concentration of 20 mM. D_2O was added to a final concentration of 10% (v/v). The solution was analyzed by ^{13}C NMR spectroscopy. Substrate/product ratios were obtained from the signals of C-4 of [1,3,4-$^{13}C_3$]-**4** (64.9 ppm) and C-4 of [1,3,4-$^{13}C_3$]-**5** (67.1 ppm).

J.3. IspE. Assay mixtures contained 100 mM Tris hydrochloride, pH 8.0, 10 mM $MgCl_2$, 1 mM dithiothreitol, 4 mM ATP, 3.4 mM [1,3,4-$^{13}C_3$]-**5**, and 0.05 U of IspE protein in a volume of 500 μL. The mixtures were incubated at 27 °C, and the reaction was terminated by the addition of EDTA to a final concentration of 20 mM. D_2O was added to a final concentration of 10% (v/v). The solution was analyzed by ^{13}C NMR spectroscopy. Substrate/product ratios were obtained from the signals of C-1 of [1,3,4-$^{13}C_3$]-**5** (66.4 ppm) and C-1 of [1,3,4-$^{13}C_3$]-**6** (65.9 ppm).

J.4. IspF. Assay mixtures contained 100 mM Tris hydrochloride, pH 8.0, 10 mM $MgCl_2$, 1 mM dithiothreitol, 3.4 mM [1,3,4-$^{13}C_3$]-**6**, and 0.05 U of IspF protein in a volume of 500 μL. The mixtures were incubated at 27 °C, and the reaction was terminated by the addition of EDTA to a final concentration of 20 mM. D_2O was added to a final concentration of 10% (v/v). The solution was analyzed by ^{13}C NMR spectroscopy. Substrate/product ratios were obtained from the signals of C-1 of [1,3,4-$^{13}C_3$]-**6** (65.9 ppm) and C-1 of [1,3,4-$^{13}C_3$]-**7** (66.8 ppm).

K. Determination of the Equilibrium Constant for the IspD Reaction. Reaction mixtures contained 150 mM Tris hydrochloride, pH 8.0, 10 mM $MgCl_2$, 10 mM dithiothreitol, 5 mM CTP, 5 mM [1,3,4-$^{13}C_3$]-**4**, and 0.3 mg of IspD protein (total volume, 1 mL). They were incubated at 37 °C and were monitored by ^{31}P NMR spectroscopy and ^{13}C NMR spectroscopy.

L. Determination of the Equilibrium Constant for the IspE Reaction. Reaction mixtures contained 150 mM Tris hydrochloride, pH 8.0, 10 mM $MgCl_2$, 10 mM dithiothreitol, 5 mM ATP, 5 mM [1,3,4-$^{13}C_3$]-**5**, and 6 mg of IspE protein (total volume, 1 mL). They were incubated at 37 °C and were monitored by ^{31}P NMR spectroscopy and ^{13}C NMR spectroscopy.

Acknowledgment. This research was made possible by NIH Grant 1 R21 NS053634-01 and the Hans-Fischer-Gesellschaft, Munich. We thank Katrin Gärtner for skillful assistance and Fritz Wendling for expert help with the preparation of the manuscript.

Supporting Information Available: Materials, high-throughput screens for IspC, IspD, IspE, and IspF, NMR spectroscopy, bacterial strains, plasmids and oligonucleotides used in this study, and a list of recombinant proteins used for screening, substrate synthesis, and as auxiliary enzymes in enzyme assays. This material is available free of charge via the Internet at http://pubs.acs.org.

JO061466O